Available online at www.sciencedirect.com
SCIENCE DIRECT®
International Journal of Mass Spectrometry 227 (2003) 235–246
International Journal of Mass Spectrometry
www.elsevier.com/locate/ijms

Gas-phase ion chemistry in silane/propyne mixtures

L. Operti*, R. Rabezzana, F. Turco, G.A. Vaglio

Dipartimento di Chimica Generale e Organica Applicata, Università degli Studi di Torino,
Corso Massimo d'Azeglio 48, 10125 Torino, Italy

Received 11 February 2003; accepted 6 March 2003

Abstract

The gas-phase ion chemistry of the silane/propyne mixture was studied by ion trap mass spectrometry with the aim of finding the best experimental conditions leading to the formation of Si- and C-containing ion clusters of increasing size. To this purpose, the optimal pressure ratio among the two gases was about 1:1. Ion/molecule reactions were investigated and rate constants determined for propyne alone and for the silane/propyne systems. In these systems, several mixed ions were formed; in particular, the $Si_2CH_5{}^+$ ion species is obtained and reaches 20% abundance after 1 s reaction time under the experimental conditions used here.

Keywords: Silane; Propyne; Ion trap mass spectrometry; Ion clusters

1. Introduction

Over the past years, several studies have been performed about the gas-phase ion chemistry of organosilicon compounds. This research area includes the study of molecules present in interstellar clouds under the effect of ionizing radiations, cosmic rays, and low wavelength photons [1,2]. Moreover, the preparation of amorphous silicon carbides, through chemical vapor deposition methods, has stimulated increasing interest, due to the semiconductive properties of the amorphous solid obtained [3–9]. As ion species are involved in the first polymerization steps, their nature and abundance give valuable suggestions about the best experimental conditions for the formation of amorphous solids of the desired composition and properties.

In the past, both experimental and theoretical studies on gas-phase ion chemistry have been performed in order to obtain information about the reactivity, reaction mechanisms, and kinetics of isolated ion species from a fundamental point of view [10–19]. The self-condensation reactions of SiH_4 have been extensively studied both experimentally [3] and theoretically [20]. Mixtures of SiH_4 with C_2H_4 and with C_2H_2 have been investigated under high pressure conditions [21,22], and ion/molecule reactions of the Si^+ ion with hydrocarbons, such as ethane, ethene, and ethyne, have already been reported [23–25].

In our laboratory, gas-phase ion/molecule reactions of SiH_4 with propene [26], ethene [27], ethane [28], ethyne [28], and allene [29] have been studied by ion trap mass spectrometry. Moreover, the ternary mixtures of silane/propene/phosphine [30] and silane/

---

* Corresponding author. Tel.: +39-0116-707-510; fax: +39-0116-707-591.
E-mail address: lorenza.operti@unito.it (L. Operti).

1387-3806/03/$ – see front matter © 2003 Elsevier Science B.V. All rights reserved.
doi:10.1016/S1387-3806(03)00124-6

propene/ammonia [31] were investigated in order to find the experimental conditions leading to formation of silicon carbides doped with phosphorus or nitrogen, which display semiconductor properties. As a development of this research, the highly unsaturated propyne molecule is reacted with silane in the present work, with the aim of investigating the overall ionic reactivity and kinetics of the silane/propyne mixture in the gas phase.

2. Experimental

All the experiments were performed in an ITMS Finnigan instrument. Silane and propyne were commercially purchased at a high purity grade and directly introduced in the inlet system. Helium buffer gas was supplied at an extra-high purity grade and used with no further purification. In all experiments using both propyne alone (self-condensation) and SiH_4/C_3H_4 mixtures, the total sample pressure was always 1.2×10^{-6} Torr (1 Torr = 133.3 Pa). The overall working pressure was approximately 8.0×10^{-5} Torr after helium introduction, as measured by a Bayard–Alpert ion gauge. The effective gas pressure is obtained from the ion gauge reading after correction for the following factors: (1) the sensitivity of the ion gauge with respect to different gases (1.7 for silane, 2.16 for propyne, and 0.2 for helium [32]), and (2) the geometry-dependent ion gauge calibration factor, determined as previously reported [4]. The temperature was set at 333 K in order to avoid thermal decomposition of the reactants.

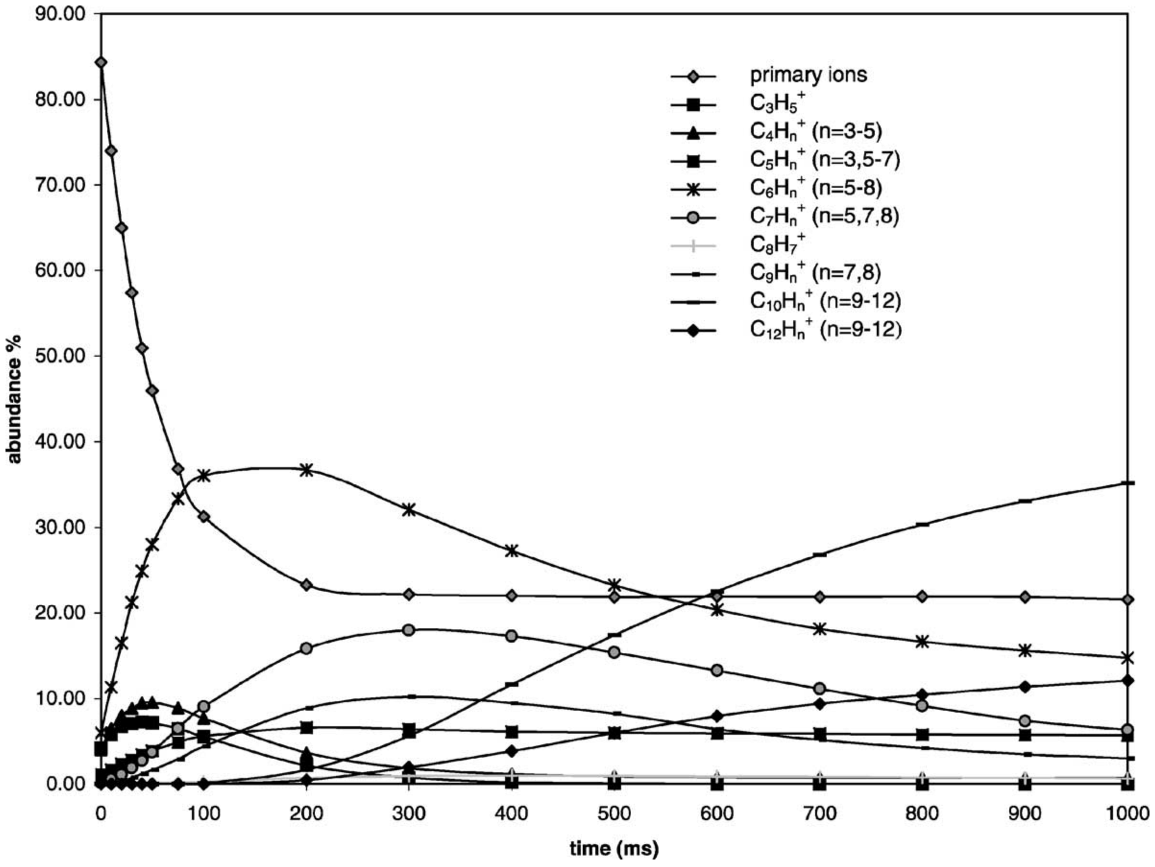

Fig. 1. Trends of the abundances of ion families vs. reaction time in propyne self-condensation experiments.

Positive ions were formed by electron ionization at about 35 eV for times in the 10–50 ms range. Ions were detected in the 14–300 u mass range. The scan functions used to investigate the reactivity of the ions (no isolation step) to derive the successive reaction paths, and to determine the kinetic constants (selective isolation steps), are described elsewhere, as well as the calculation procedures [14–16,33]. The first step of investigation consists of reaction of the ionized gaseous mixture for a suitable reaction time (usually ranging from 0 to 1 s) in order to detect the main ion species formed and to follow the variation of their abundances with reaction time. In successive experiments, all the ions formed with enough abundance (ca. 2%) are isolated by superimposition of rf and dc voltages and reacted with the neutral molecules in order to identify the ion products and to measure the rate constants of the main processes observed. This procedure was followed for the study of both self-condensation of propyne and reactions of silane/propyne systems. In this latter case, several signals were observed which could be attributed to two different isobaric species, e.g., at *m*/*z* 42 ($C_3H_6^+$ and $SiCH_2^+$). When two isobaric species can be hypothesized from reactions of a selected ion with the two neutrals, experiments performed by varying the pressure of one reagent and keeping the other one constant often allowed to rule out the formation of one of the two possible ions. If both the isobaric species were formed, the double isolation method could permit to selectively isolate each of them. This method consists of selecting a precursor ion which reacts to give only one among two or more isobaric ions. If the suitable precursor is available, its selection and reaction yields the desired

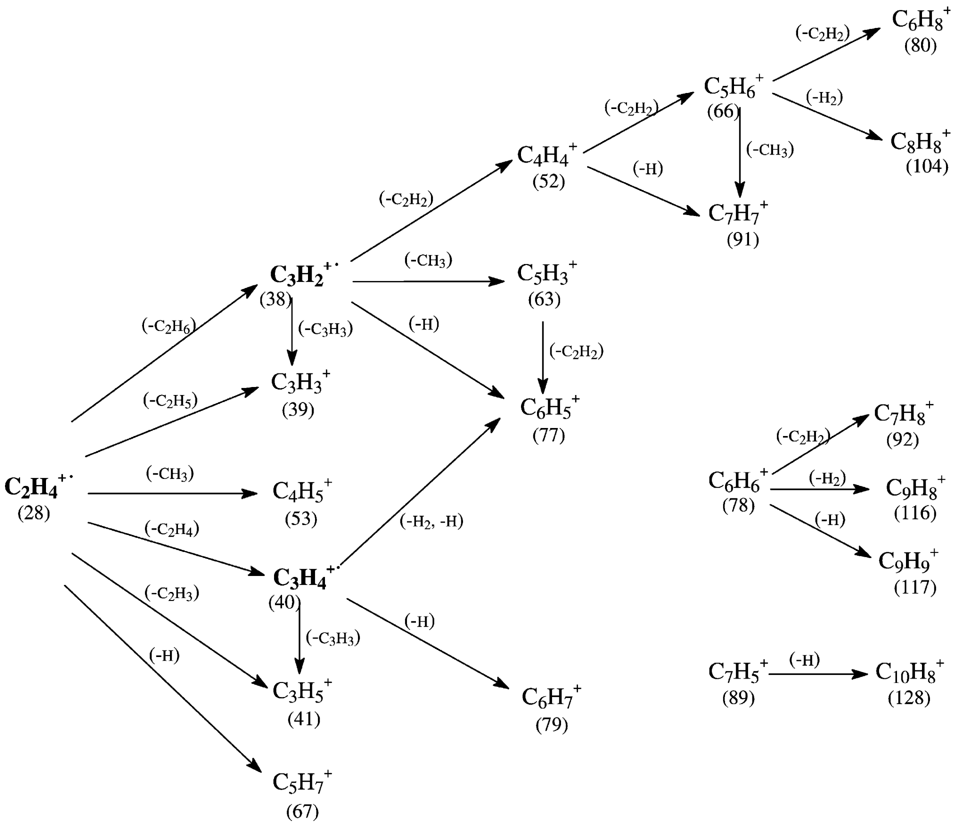

Scheme 1.

ion which may in turn be isolated and reacted. This multiple-stage isolation method may be extended up to the second step only, as the abundances of the ions decrease with increasing number of isolation steps.

3. Results and discussion

3.1. Propyne

Ionization of propyne with 35 eV electrons gives the primary $C_3H_n^+$ ($n = 0$–4) and fragment $C_2H_n^+$ ($n = 3$ and 4) ion species, which react with propyne to give several charged species of higher mass. Fig. 1 shows the trends of the abundances vs. reaction time for ion families with the same number of C atoms. The overall abundance of the primary ions rapidly decreases up to 200 ms, and then levels out. This may be ascribed to the fact that some primary ions, apart from reacting, are also formed in ion/molecule reactions (as an example, $C_2H_4^+$ yields the $C_3H_{2-4}^+$ ions). Moreover, it may be observed that heavy ions are formed with good abundances and, in fact, the $C_{10}H_n^+$ ion family is the most abundant after 600 ms reaction time. Schemes 1 and 2 report the reactions originated from primary ions of propyne with odd and even number of electrons, respectively (primary ions are in bold characters). Moreover, in Scheme 1 the successive reaction steps of secondary ions with an even number of hydrogen atoms are shown, whereas Scheme 2 displays the paths from ions with an odd number of hydrogens. The $C_3H_5^+$, $C_6H_5^+$, and $C_6H_7^+$ ions are rapidly formed with appreciable abundances (Schemes 1

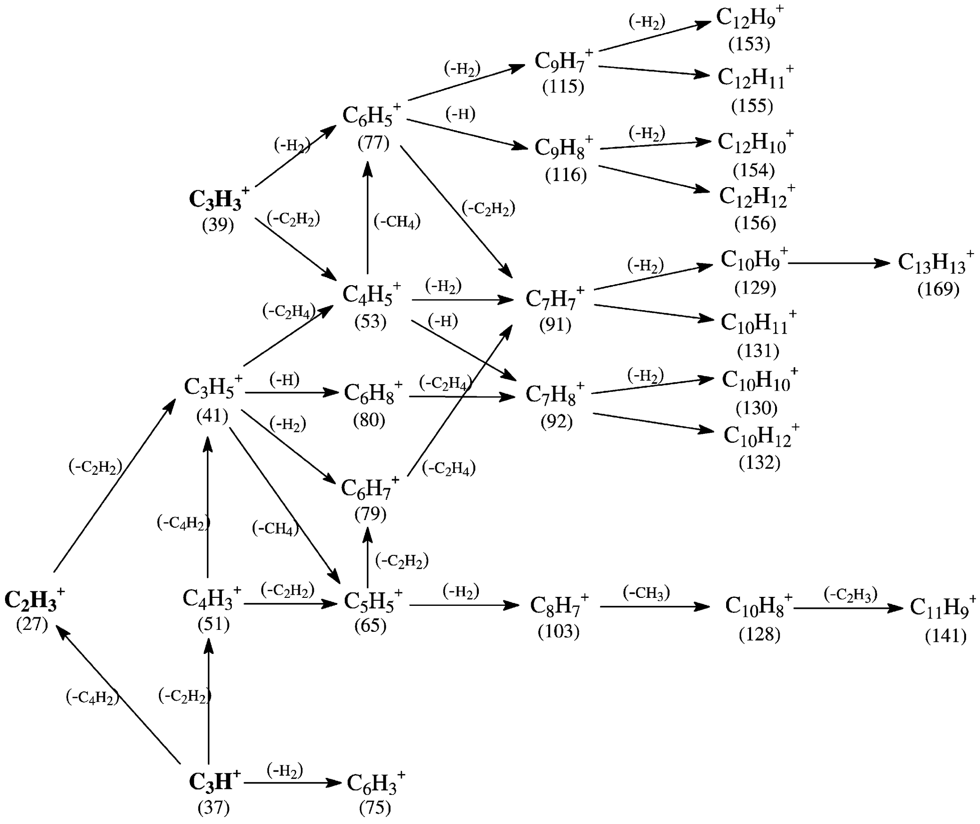

Scheme 2.

Table 1
Ion/molecule reactions in propyne[a]

Reaction	k_{exp}	$\sum k_{exp}$	$k_{collisional}$[b]	Efficiency[c]
$C_2H_3^+ + C_3H_4 \rightarrow C_3H_5^+ + C_2H_2$	9.5	9.5	17.42	0.54
$C_2H_4^+ + C_3H_4 \rightarrow C_3H_2^+ + C_2H_6$	0.58			
$C_2H_4^+ + C_3H_4 \rightarrow C_3H_3^+ + C_2H_5$	9.9			
$C_2H_4^+ + C_3H_4 \rightarrow C_3H_4^+ + C_2H_4$	0.53			
$C_2H_4^+ + C_3H_4 \rightarrow C_3H_5^+ + C_2H_3$	0.54			
$C_2H_4^+ + C_3H_4 \rightarrow C_4H_5^+ + CH_3$	0.31	11.9	17.23	0.69
$C_3H^+ + C_3H_4 \rightarrow C_2H_3^+ + C_4H_2$	1.6			
$C_3H^+ + C_3H_4 \rightarrow C_4H_3^+ + C_2H_2$	9.4			
$C_3H^+ + C_3H_4 \rightarrow C_6H_3^+ + H_2$	0.28	11.3	15.96	0.71
$C_3H_2^+ + C_3H_4 \rightarrow C_3H_3^+ + C_3H_3$	1.5			
$C_3H_2^+ + C_3H_4 \rightarrow C_4H_4^+ + C_2H_2$	5.3			
$C_3H_2^+ + C_3H_4 \rightarrow C_5H_3^+ + CH_3$	0.59			
$C_3H_2^+ + C_3H_4 \rightarrow C_6H_5^+ + H$	1.3	8.7	15.85	0.55
$C_3H_3^+ + C_3H_4 \rightarrow C_4H_5^+ + C_2H_2$	0.32			
$C_3H_3^+ + C_3H_4 \rightarrow C_6H_5^+ + H_2$	1.5	1.8	15.74	0.11
$C_3H_4^+ + C_3H_4 \rightarrow C_3H_5^+ + C_3H_3$	0.80			
$C_3H_4^+ + C_3H_4 \rightarrow C_6H_5^+ + H_2 + H$	0.55			
$C_3H_4^+ + C_3H_4 \rightarrow C_6H_7^+ + H$	5.1	6.4	15.64	0.41
$C_3H_5^+ + C_3H_4 \rightarrow C_4H_5^+ + C_2H_4$	1.1			
$C_3H_5^+ + C_3H_4 \rightarrow C_5H_5^+ + CH_4$	0.20			
$C_3H_5^+ + C_3H_4 \rightarrow C_6H_7^+ + H_2$	2.8			
$C_3H_5^+ + C_3H_4 \rightarrow C_6H_8^+ + H$	0.78	4.9	15.54	0.31
$C_4H_3^+ + C_3H_4 \rightarrow C_3H_5^+ + C_4H_2$	1.0			
$C_4H_3^+ + C_3H_4 \rightarrow C_5H_5^+ + C_2H_2$	5.0	6.0	14.77	0.41
$C_4H_4^+ + C_3H_4 \rightarrow C_7H_7^+ + H$	6.5	6.5	14.71	0.44
$C_4H_5^+ + C_3H_4 \rightarrow C_6H_5^+ + CH_4$	1.9			
$C_4H_5^+ + C_3H_4 \rightarrow C_7H_7^+ + H_2$	1.1			
$C_4H_5^+ + C_3H_4 \rightarrow C_7H_8^+ + H$	0.32	3.3	14.65	0.22
$C_5H_3^+ + C_3H_4 \rightarrow C_6H_5^+ + C_2H_2$	0.95	0.95	14.14	0.067
$C_5H_5^+ + C_3H_4 \rightarrow C_6H_7^+ + C_2H_2$	1.3			
$C_5H_5^+ + C_3H_4 \rightarrow C_8H_7^+ + H_2$	0.50	1.8	14.06	0.13
$C_6H_5^+ + C_3H_4 \rightarrow C_7H_7^+ + C_2H_2$	1.2			
$C_6H_5^+ + C_3H_4 \rightarrow C_9H_7^+ + H_2$	2.5			
$C_6H_5^+ + C_3H_4 \rightarrow C_9H_8^+ + H$	0.38	4.1	13.63	0.30
$C_6H_6^+ + C_3H_4 \rightarrow C_7H_8^+ + C_2H_2$	0.36			
$C_6H_6^+ + C_3H_4 \rightarrow C_9H_8^+ + H_2$	0.94	1.3	13.60	0.096
$C_6H_7^+ + C_3H_4 \rightarrow C_7H_7^+ + C_2H_4$	0.20	0.20	13.57	0.015
$C_6H_8^+ + C_3H_4 \rightarrow C_7H_8^+ + C_2H_4$	0.24	0.24	13.54	0.018
$C_7H_7^+ + C_3H_4 \rightarrow C_{10}H_9^+ + H_2$	0.18	0.18	13.27	0.014
$C_7H_8^+ + C_3H_4 \rightarrow C_{10}H_{10}^+ + H_2$	0.44			
$C_7H_8^+ + C_3H_4 \rightarrow C_{10}H_{12}^+$	0.62	1.1	13.25	0.083
$C_9H_7^+ + C_3H_4 \rightarrow C_{12}H_9^+ + H_2$	0.23			
$C_9H_7^+ + C_3H_4 \rightarrow C_{12}H_{11}^+$	0.32	0.55	12.84	0.043

[a] Rate constants are expressed as 10^{-10} cm^3 molecule^{-1} s^{-1}; uncertainty is within 20%.

[b] Collisional rate constants have been calculated according to the Parametrized Trajectory Theory [35] taking the polarizability and the dipole moment of propyne from refs. [36] and [37], respectively.

[c] Efficiency has been calculated as the ratio $\sum k_{exp}/k_{collisional}$.

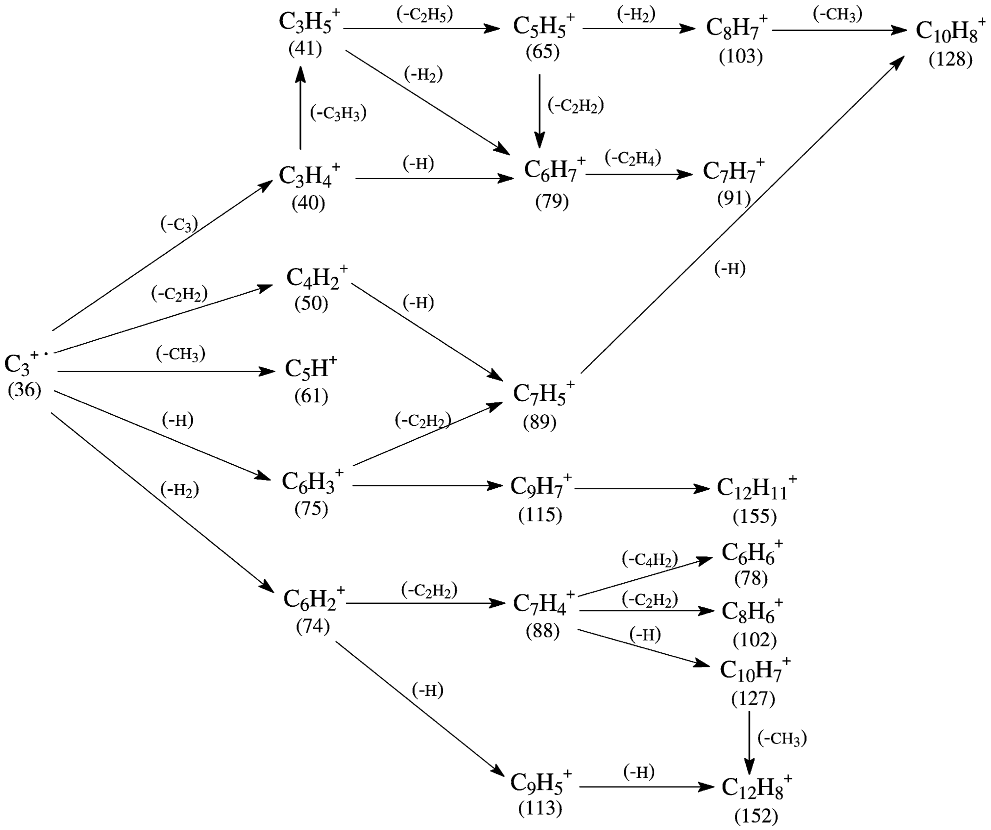

Scheme 3.

and 2), and in turn react to give, through multiple reaction steps, the heaviest ions detected under the present experimental conditions, such as $C_{12}H_{12}^+$ and $C_{13}H_{13}^+$ (Scheme 2). Scheme 1 also reports reactions of the $C_6H_6^+$ and $C_7H_5^+$ ion species. Both ions are formed through several low efficiency pathways, each of them never exceeding 2% of abundance. However, at long reaction times their total abundance is high enough to allow their selection and reaction.

The reactions originated from the C_3^+ (m/z 36) ions are reported in a separate scheme (Scheme 3) for sake of clarity because of the large number of pathways detected. Moreover, as the non-hydrogenated C_3^+ ion species is little abundant and very reactive, as well as the ions produced in the following steps, the determination of rate constants of the processes was not possible.

Experimental and collisional rate constants, and reaction efficiencies of the main reactions taking place after ionization of propyne, are reported in Table 1. In agreement with literature data [34], most of the high rate constants ($k > 5.0 \times 10^{-10}$ cm^3 molecule^{-1} s^{-1}) are referred to reactions in which the neutral loss is C_2H_2 or H, the former being characteristic of highly unsaturated species, and the latter of the less unsaturated ones. Reactions of the secondary ions are generally less efficient with respect to those of the primary ion species. The high mass ions mainly react to give association products, with low rate constants.

3.2. Silane/propyne

Three different SiH_4/C_3H_4 mixtures with pressure ratios of 1:1, 1:5, and 5:1 and total pressure of about

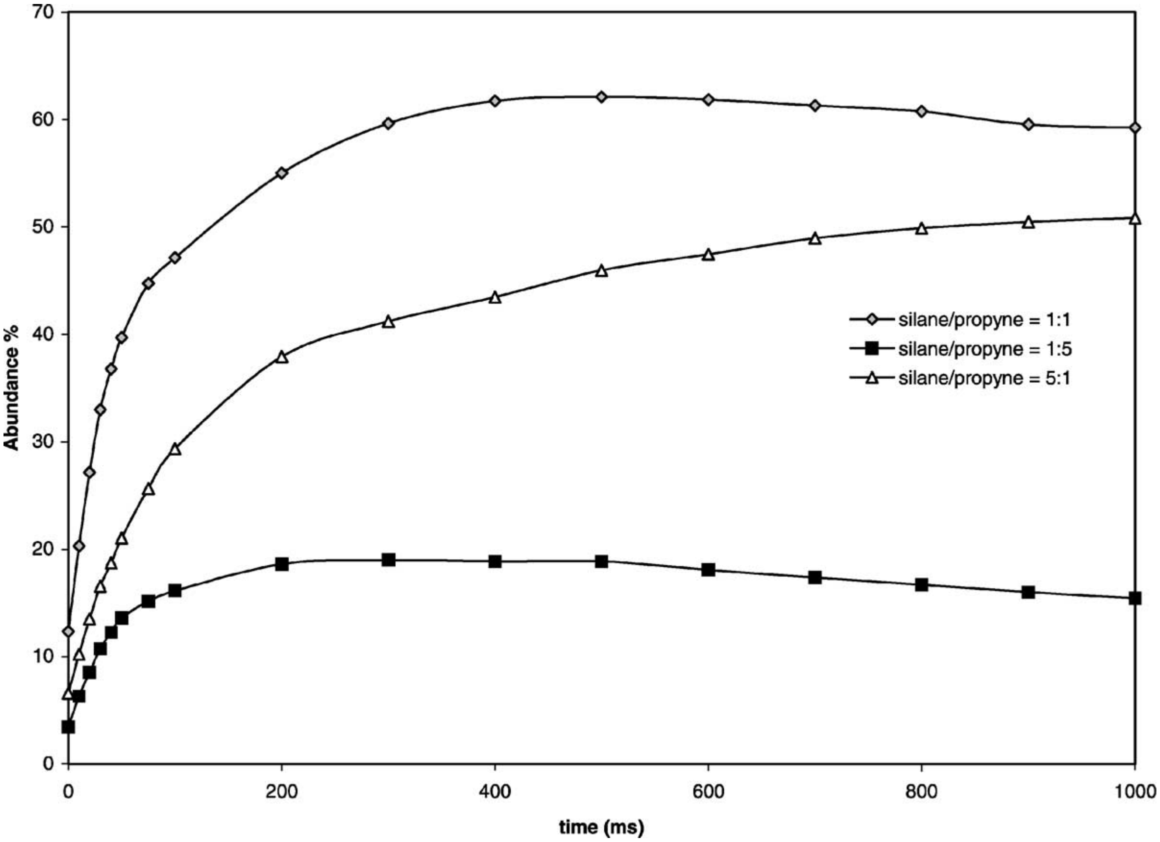

Fig. 2. Trends of the abundances of Si- and C-containing ions in three different SiH_4/C_3H_4 mixtures, with partial pressure ratios of 1:1, 1:5, and 5:1, respectively.

1.2×10^{-6} Torr were reacted up to 1 s, in order to determine which pressure ratio gave the best yield of mixed ion species. The variation of the abundances of ions containing both carbon and silicon atoms vs. time is reported in Fig. 2 for the three mixtures. The highest yield is reached in the SiH_4/C_3H_4 1:1 system, and hence this pressure ratio was adopted in the following experiments. The lowest yield of mixed ions in the SiH_4/C_3H_4 1:5 mixtures is probably due to the more favored self-condensation processes of propyne with respect to reactions with silane. Table 2 reports the percentage abundances of the main ions observed in the SiH_4/C_3H_4 1:1 mixture at different reaction times ranging from 0 to 1 s. As several isobaric ions are formed in these processes (in parentheses are the less abundant species, as evidenced by ion isolation experiments), it was not possible to report in a plot the abundances of all ion families vs. time. Therefore, the trends of ion abundances vs. reaction time shown in Fig. 3 only concern the most abundant ion species, which exceed the arbitrarily set threshold of 5%, and are almost exclusively mixed ions. At low reaction times (<100 ms), the most abundant ions are at *m*/*z* 45 ($SiCH_5^+$), 59 ($Si_2H_3^+$, $SiC_2H_7^+$), 67 ($SiC_3H_3^+$), and 79 ($C_6H_7^+$), with abundances of about 6–8%. The contribution to the peak at *m*/*z* 59 of $Si_2H_3^+$ is roughly estimated by comparison with self-condensation experiments, and the remaining abundance is assigned to the $SiC_2H_7^+$ ion, which is the only one among the two isobaric species that exceeds the 5% threshold abundance. At longer reaction times, the abundance of the isobaric ions $Si_2CH_5^+$ and $SiC_3H_9^+$ at *m*/*z* 73

Table 2
Relative abundances of significant ions in the ion trap mass spectra of the SiH_4/C_3H_4 1:1 mixture as a function of the reaction time

Ion	Reaction time (ms)									
	0	30	50	75	100	300	500	700	900	1000
$C_2H_3^+$	3.13	0.60	0.30	0.14	–	–	–	–	–	–
$C_2H_4^+$, Si^+	4.59	1.51	0.86	0.46	0.25	–	–	–	–	–
SiH^+, $(C_2H_5^+)$	4.57	3.02	1.90	1.07	0.64	–	–	–	–	–
SiH_2^+	10.25	4.62	2.52	1.53	0.95	–	–	–	–	–
SiH_3^+	11.15	7.80	5.39	3.30	2.13	0.10	–	–	–	–
C_3H^+	3.98	1.38	0.85	0.80	0.87	0.68	0.67	0.61	0.64	0.59
$C_3H_2^+$	6.56	2.56	1.90	1.62	1.53	1.42	1.10	1.24	1.10	1.16
$C_3H_3^+$	18.8	15.0	11.5	9.44	8.09	5.60	5.45	5.63	5.86	5.96
$C_3H_4^+$	14.99	4.77	4.16	3.43	2.86	1.95	2.05	2.16	2.25	2.30
$C_3H_5^+$	2.82	4.00	3.80	2.88	2.53	1.54	1.26	1.25	1.25	1.23
$SiCH_2^+$, $C_3H_6^+$	0.93	1.86	2.05	1.83	1.44	0.59	0.41	0.30	0.23	0.21
$SiCH_3^+$	1.74	4.97	5.69	5.77	5.37	1.91	0.93	0.58	0.34	0.34
$SiCH_4^+$	1.24	2.51	2.29	2.26	2.12	0.69	0.34	0.24	0.19	0.19
$SiCH_5^+$	2.15	7.55	8.68	8.29	7.15	1.46	0.67	0.66	0.77	0.82
$C_4H_3^+$	0.71	1.32	1.24	0.99	0.70	0.11	–	–	–	–
$C_4H_4^+$	0.65	1.33	1.35	1.19	0.94	0.39	0.16	–	–	–
$C_4H_5^+$	0.82	1.87	1.99	2.03	1.93	0.50	0.28	0.16	0.15	0.12
$C_4H_6^+$, $(SiC_2H_2^+)$	0.27	0.66	0.54	0.68	0.72	0.33	0.15	–	–	–
$SiC_2H_3^+$	1.28	2.76	2.90	2.73	2.46	1.17	0.52	0.23	0.16	–
$SiC_2H_4^+$, $(C_4H_8^+)$	0.16	0.51	0.55	0.65	0.68	0.45	0.19	–	–	–
$SiC_2H_5^+$	0.50	1.06	1.16	0.92	0.79	1.12	0.45	0.18	–	–
$Si_2H_2^+$, $(SiC_2H_6^+)$	0.76	1.96	2.25	1.99	1.51	0.96	0.28	–	–	–
$SiC_2H_7^+$, $(Si_2H_3^+)$	0.56	3.19	5.17	7.51	8.88	3.90	1.13	0.43	0.23	0.22
$Si_2H_4^+$	0.74	1.78	1.80	1.48	2.03	1.09	0.27	–	–	–
$Si_2H_5^+$	0.17	0.47	0.54	0.53	0.53	0.54	0.17	–	–	–
$C_5H_3^+$	0.19	0.35	0.35	0.34	0.33	0.25	0.24	0.23	0.23	0.21
$C_5H_5^+$	0.32	0.75	0.97	1.16	1.28	1.10	1.12	1.11	1.05	1.02
$SiC_3H_2^+$, $(C_5H_6^+)$	0.32	0.80	0.94	0.66	0.78	1.35	1.34	1.31	1.22	1.20
$SiC_3H_3^+$	1.25	4.30	5.74	7.08	7.70	6.07	5.38	5.12	4.85	4.79
$SiC_3H_4^+$	0.30	0.86	1.16	1.38	1.39	1.65	1.56	1.50	1.47	1.44
$SiC_3H_5^+$	0.80	2.59	3.28	3.78	3.73	1.59	0.95	0.84	0.82	0.80
$SiC_3H_6^+$, $Si_2CH_2^+$	0.17	0.52	0.66	0.68	0.72	0.89	1.70	1.96	2.14	2.27
$SiC_3H_7^+$	0.25	0.80	1.00	1.15	1.13	0.92	1.19	1.67	1.83	1.84
$Si_2CH_5^+$, $(SiC_3H_9^+)$	–	0.21	0.61	1.55	3.00	16.4	19.9	20.3	20.3	20.5
$Si_2CH_6^+$	–	0.14	0.19	0.27	0.38	3.97	5.98	6.48	6.60	6.62
$Si_2CH_7^+$	–	0.12	0.17	0.23	0.28	0.76	1.23	1.75	2.07	2.17
$C_6H_5^+$	0.81	2.30	2.58	2.52	2.23	0.78	0.43	0.38	0.40	0.37
$C_6H_7^+$	1.75	4.75	5.91	6.73	7.22	6.39	4.74	3.86	3.36	3.14
$C_6H_8^+$	0.10	0.30	0.41	0.50	0.54	1.24	1.27	1.10	0.97	0.91
$SiC_4H_5^+$	–	0.33	0.73	1.28	1.77	2.10	1.12	0.78	0.59	0.52
$SiC_4H_7^+$, $Si_2C_2H_3^+$	–	0.42	0.78	1.24	1.59	1.71	0.99	0.60	0.41	0.36
$SiC_4H_9^+$, $Si_2C_2H_5^+$	–	0.10	0.20	0.39	0.55	0.94	0.55	0.29	0.18	0.12
$C_7H_7^+$	–	0.39	0.82	1.32	1.76	3.11	2.88	2.58	2.25	2.05
$C_7H_8^+$	–	–	–	–	0.14	0.37	0.84	1.11	1.20	1.21

increases and becomes the highest after about 200 ms of reaction. By considering ions of the same families, i.e., $Si_2CH_6^+$ and $SiC_3H_3^+$, respectively, and their variation of abundance with reaction time, it is evident that the trend of *m*/*z* 73 is more similar to that of $Si_2CH_6^+$. In fact, it increases and reaches a plateau at, more or less, the same time of the *m*/*z* 74 curve, whereas the abundance of $SiC_3H_3^+$ reaches a

Table 3
Ion/molecule reactions of the $Si_nH_m{}^+$ ions with propyne and of the $C_mH_n{}^+$ ions with silane[a]

Reaction	k_{exp}	$\sum k_{exp}$	$k_{collisional}$[b]	Efficiency[c]
$SiH^+ + C_3H_4 \rightarrow SiCH_3{}^+ + C_2H_2$	14			
$SiH^+ + C_3H_4 \rightarrow SiC_3H_3{}^+ + H_2$	0.76			
$SiH^+ + C_3H_4 \rightarrow SiC_3H_4{}^+ + H$	0.53	15	17.05	0.90
$SiH_2{}^+ + C_3H_4 \rightarrow SiH_3{}^+ + C_3H_3$	5.0			
$SiH_2{}^+ + C_3H_4 \rightarrow SiCH_2{}^+ + C_2H_4$	3.7			
$SiH_2{}^+ + C_3H_4 \rightarrow SiCH_4{}^+ + C_2H_2$	1.2			
$SiH_2{}^+ + C_3H_4 \rightarrow SiC_2H_3{}^+ + CH_3$	5.2			
$SiH_2{}^+ + C_3H_4 \rightarrow SiC_3H_3{}^+ + H_2 + H$	0.37			
$SiH_2{}^+ + C_3H_4 \rightarrow SiC_3H_5{}^+ + H$	2.8	18.3	16.88	1.08
$SiH_3{}^+ + C_3H_4 \rightarrow SiCH_3{}^+ + C_2H_4$	1.2			
$SiH_3{}^+ + C_3H_4 \rightarrow SiCH_5{}^+ + C_2H_2$	12	13	16.73	0.78
$Si_2H_3{}^+ + C_3H_4 \rightarrow SiCH_3{}^+ + SiC_2H_4$	1.6			
$Si_2H_3{}^+ + C_3H_4 \rightarrow SiC_3H_5{}^+ + SiH_2$ and/or $Si_2CH^+ + C_2H_6$	0.60			
$Si_2H_3{}^+ + C_3H_4 \rightarrow Si_2CH_3{}^+ + C_2H_4$ and/or $SiC_3H_7{}^+ + Si$	1.7			
$Si_2H_3{}^+ + C_3H_4 \rightarrow Si_2CH_5{}^+ + C_2H_2$	0.70			
$Si_2H_3{}^+ + C_3H_4 \rightarrow Si_2C_3H_3{}^+ + 2H_2$	0.77			
$Si_2H_3{}^+ + C_3H_4 \rightarrow Si_2C_3H_5{}^+ + H_2$	0.78	6.2	14.32	0.43
$Si_2H_4{}^+ + C_3H_4 \rightarrow SiC_3H_5{}^+ + SiH_3$	4.2			
$Si_2H_4{}^+ + C_3H_4 \rightarrow Si_2CH_4{}^+ + C_2H_4$	1.4			
$Si_2H_4{}^+ + C_3H_4 \rightarrow Si_2CH_5{}^+ + C_2H_3$	0.68			
$Si_2H_4{}^+ + C_3H_4 \rightarrow Si_2CH_6{}^+ + C_2H_2$	0.60	6.9	14.27	0.48
$Si_2H_5{}^+ + C_3H_4 \rightarrow SiC_3H_5{}^+ + SiH_4$	0.71			
$Si_2H_5{}^+ + C_3H_4 \rightarrow SiC_3H_6{}^+ + SiH_3$	0.34			
$Si_2H_5{}^+ + C_3H_4 \rightarrow Si_2CH_5{}^+ + C_2H_4$	1.4			
$Si_2H_5{}^+ + C_3H_4 \rightarrow Si_2CH_7{}^+ + C_2H_2$	2.7	5.2	14.23	0.36
$C_3H^+ + SiH_4 \rightarrow SiCH_3{}^+ + C_2H_2$	3.4			
$C_3H^+ + SiH_4 \rightarrow SiC_3H_2{}^+ + H_2 + H$	1.6			
$C_3H^+ + SiH_4 \rightarrow SiC_3H_3{}^+ + H_2$	1.9	6.9	11.75	0.59
$C_3H_2{}^+ + SiH_4 \rightarrow SiCH_3{}^+ + C_2H_3$	1.2			
$C_3H_2{}^+ + SiH_4 \rightarrow SiC_2H_3{}^+ + CH_3$	0.92			
$C_3H_2{}^+ + SiH_4 \rightarrow SiC_3H_3{}^+ + H_2 + H$	0.86			
$C_3H_2{}^+ + SiH_4 \rightarrow SiC_3H_5{}^+ + H$	0.39	3.4	11.68	0.29
$C_3H_3{}^+ + SiH_4 \rightarrow SiCH_5{}^+ + C_2H_2$	0.50	0.50	11.61	0.043
$C_3H_4{}^+ + SiH_4 \rightarrow SiCH_4{}^+ + C_2H_4$	2.3			
$C_3H_4{}^+ + SiH_4 \rightarrow SiC_2H_5{}^+ + CH_3$	0.77			
$C_3H_4{}^+ + SiH_4 \rightarrow SiC_3H_7{}^+ + H$	0.40	3.5	11.54	0.30
$C_3H_5{}^+ + SiH_4 \rightarrow SiCH_5{}^+ + C_2H_4$	1.3	1.3	11.48	0.11
$C_4H_3{}^+ + SiH_4 \rightarrow SiC_2H_5{}^+ + C_2H_2$	0.45	0.45	10.98	0.041

[a] Rate constants are expressed as 10^{-10} cm^3 molecule^{-1} s^{-1}; uncertainty is within 20%.

[b] Collisional rate constants have been calculated according to the Parametrized Trajectory Theory [35] taking the polarizability of propyne from ref. [36] and that of silane from ref. [38] and the dipole moment of propyne from ref. [37].

[c] Efficiency has been calculated as the ratio $\sum k_{exp}/k_{collisional}$.

maximum at a shorter reaction time and then decreases. Such behavior suggests that the signal at *m*/*z* 73 is mainly due to the $Si_2CH_5{}^+$ ion species. Further, it is quite unlikely that the unsaturated propyne can originate a highly hydrogenated abundant species, such as $SiC_3H_9{}^+$.

Table 3 displays the reaction rate constants of ions from silane with propyne and of ions from propyne with silane, while Table 4 reports the reaction rate constants of mixed ions with both propyne and silane. Collisional rate constants and reaction efficiencies are also reported in the tables. Ions from silane react with

Table 4
Ion/molecule reactions of the $\mathrm{Si}_n\mathrm{C}_m\mathrm{H}_l{}^+$ ions with propyne and silane[a]

Reaction	k_{exp}	$\sum k_{\mathrm{exp}}$	$k_{\mathrm{collisional}}$[b]	Efficiency[c]
$\mathrm{SiCH_2{}^+ + C_3H_4 \rightarrow SiC_2H_2{}^+ + C_2H_4}$	0.82			
$\mathrm{SiCH_2{}^+ + C_3H_4 \rightarrow SiC_3H_3{}^+ + CH_3}$	10			
$\mathrm{SiCH_2{}^+ + C_3H_4 \rightarrow SiC_3H_4{}^+ + CH_2}$	0.32			
$\mathrm{SiCH_2{}^+ + C_3H_4 \rightarrow SiC_4H_5{}^+ + H}$	1.0	12	15.45	0.78
$\mathrm{SiCH_2{}^+ + SiH_4 \rightarrow Si_2CH_4{}^+ + H_2}$	2.2	2.2	11.42	0.19
$\mathrm{SiCH_3{}^+ + C_3H_4 \rightarrow SiC_2H_3{}^+ + C_2H_4}$	1.2			
$\mathrm{SiCH_3{}^+ + C_3H_4 \rightarrow SiC_4H_5{}^+ + H}$	1.4	2.6	15.36	0.17
$\mathrm{SiCH_4{}^+ + C_3H_4 \rightarrow SiCH_3{}^+ + C_3H_5}$	0.68			
$\mathrm{SiCH_4{}^+ + C_3H_4 \rightarrow SiC_2H_4{}^+ + C_2H_4}$	1.0			
$\mathrm{SiCH_4{}^+ + C_3H_4 \rightarrow SiC_2H_6{}^+ + C_2H_2}$	1.6			
$\mathrm{SiCH_4{}^+ + C_3H_4 \rightarrow SiC_3H_5{}^+ + CH_3}$	3.8			
$\mathrm{SiCH_4{}^+ + C_3H_4 \rightarrow SiC_4H_6{}^+ + H_2}$	0.41			
$\mathrm{SiCH_4{}^+ + C_3H_4 \rightarrow SiC_4H_7{}^+ + H}$	0.81	8.3	15.28	0.54
$\mathrm{SiCH_4{}^+ + SiH_4 \rightarrow SiCH_5{}^+ + SiH_3}$	2.0			
$\mathrm{SiCH_4{}^+ + SiH_4 \rightarrow Si_2H_3{}^+ + CH_4 + H}$	0.69	2.7	11.30	0.24
$\mathrm{SiCH_5{}^+ + C_3H_4 \rightarrow SiC_2H_7{}^+ + C_2H_2}$	9.9	9.9	15.20	0.65
$\mathrm{SiC_2H_3{}^+ + C_3H_4 \rightarrow SiC_3H_3{}^+ + C_2H_4}$	1.3			
$\mathrm{SiC_2H_3{}^+ + C_3H_4 \rightarrow SiC_3H_5{}^+ + C_2H_2}$	1.9			
$\mathrm{SiC_2H_3{}^+ + C_3H_4 \rightarrow SiC_5H_5{}^+ + H_2}$	2.1	5.3	14.53	0.36
$\mathrm{SiC_2H_5{}^+ + C_3H_4 \rightarrow SiC_3H_5{}^+ + C_2H_4}$	1.2			
$\mathrm{SiC_2H_5{}^+ + C_3H_4 \rightarrow SiC_3H_7{}^+ + C_2H_2}$	3.5			
$\mathrm{SiC_2H_5{}^+ + C_3H_4 \rightarrow SiC_5H_7{}^+ + H_2}$	1.7	6.4	14.42	0.44
$\mathrm{SiC_2H_7{}^+ + C_3H_4 \rightarrow SiC_3H_9{}^+ + C_2H_2}$	7.5	7.5	14.32	0.52
$\mathrm{SiC_3H_2{}^+ + C_3H_4 \rightarrow SiC_6H_5{}^+ + H}$	4.8	4.8	14.02	0.34
$\mathrm{SiC_3H_5{}^+ + C_3H_4 \rightarrow SiC_4H_5{}^+ + C_2H_4}$	2.3			
$\mathrm{SiC_3H_5{}^+ + C_3H_4 \rightarrow SiC_4H_7{}^+ + C_2H_2}$	1.3	3.6	13.90	0.26
$\mathrm{SiC_3H_7{}^+ + C_3H_4 \rightarrow SiC_4H_7{}^+ + C_2H_4}$	1.9			
$\mathrm{SiC_3H_7{}^+ + C_3H_4 \rightarrow SiC_4H_9{}^+ + C_2H_2}$	2.0			
$\mathrm{SiC_3H_7{}^+ + C_3H_4 \rightarrow SiC_6H_9{}^+ + H_2}$	2.0	5.9	13.83	0.43
$\mathrm{SiC_4H_5{}^+ + C_3H_4 \rightarrow SiCH_3{}^+ + C_6H_6}$	1.4			
$\mathrm{SiC_4H_5{}^+ + C_3H_4 \rightarrow SiC_7H_7{}^+ + H_2}$	2.3	3.7	13.52	0.27
$\mathrm{SiC_4H_5{}^+ + SiH_4 \rightarrow Si_2C_2H_5{}^+ + C_2H_4}$	0.86			
$\mathrm{SiC_4H_5{}^+ + SiH_4 \rightarrow Si_2C_4H_7{}^+ + H_2}$	0.91	1.77	10.16	0.17

[a] Rate constants are expressed as $10^{-10}\,\mathrm{cm^3\,molecule^{-1}\,s^{-1}}$; uncertainty is within 20%.

[b] Collisional rate constants have been calculated according to the Parametrized Trajectory Theory [35] taking the polarizability of propyne from ref. [36] and that of silane from ref. [38] and the dipole moment of propyne from ref. [37].

[c] Efficiency has been calculated as the ratio $\sum k_{\mathrm{exp}}/k_{\mathrm{collisional}}$.

propyne with very high efficiency for the light ions and lower for the heavy ion species. Condensation reactions are frequently observed, and are followed by hydrocarbon or hydrogen, both as atom and molecule, neutral loss. In reactions of propyne ions with neutral silane, the efficiency is never very high; a lower number of pathways are observed and hydrocarbon radicals or molecules are the most frequent neutral losses. This behavior is in agreement with the higher reactivity of the unsaturated propyne towards cations, with respect to silane. The same trend is observed for mixed ions, which preferably react with propyne, giving ion clusters with increasing number of carbon atoms (Table 4). It is worth noting that the $\mathrm{SiCH_3{}^+}$ ion yields $\mathrm{SiC_4H_5{}^+}$ and vice versa through different reactions, thus introducing an error in the calculation of the respective rate constants, which is evaluated to be lower than 50%. In all other cases, uncertainty in the rate constants measurements is within 20%. Due to mass overlapping, the reactivity of some ion species, such as $\mathrm{Si^+}$ and $\mathrm{C_2H_4{}^+}$

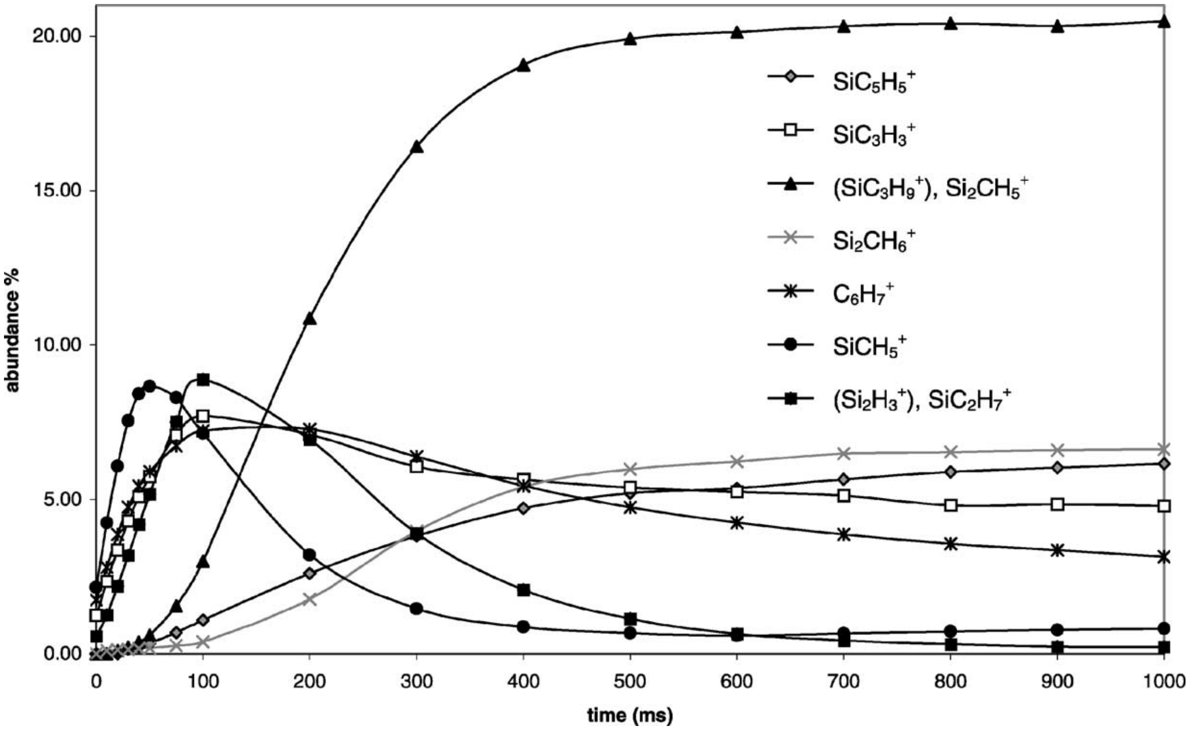

Fig. 3. Trends of the abundances of ions families whose abundance exceed the 5% threshold in the SiH_4/C_3H_4 1:1 mixture.

(*m*/*z* 28), was not studied as no experiment could afford the isolation of only one of the two ions. In other cases, the double isolation method allowed to select a single isobaric ion, provided that its abundance was high enough to get an appreciable signal-to-noise ratio. This condition is not always fulfilled, and this is the reason why some ions do not appear in the table.

4. Conclusions

Ion/molecule reactions in propyne and in the silane/propyne mixtures have been studied by ion trap mass spectrometry and experimental rate constants for the main processes were calculated. The high reactivity of propyne towards positive ions, due to the presence of two π-electron pairs, leads to the formation of several ion products with high efficiencies, even if each rate constant is generally rather low. In the binary mixture, most of the fast processes lead to formation of mixed ions, and this is encouraging in view of the synthesis of silicon carbides from appropriate gaseous mixtures. The 1:1 pressure ratio among silane and propyne gives the highest yield of mixed ions. In particular, the most abundant species are $SiCH_n^+$ ($n = 2$–5), $SiC_2H_n^+$ ($n = 2$–7), and $SiC_3H_n^+$ ($n = 2$–7) for reaction times up to 150 ms, and subsequently, the $Si_2CH_n^+$ ($n = 2$, 4–7) ion family. Comparison with silane/hydrocarbon systems previously studied [26–29] confirms the attitude of Si- and C-containing ions to preferably react with the unsaturated hydrocarbon molecules, leading to mixed ions with increasing content of C with respect to Si. In a previous paper [26b], it was demonstrated by means of B3LYP calculations that silicon-containing ions preferably react with propene with respect to silane, due to the higher entropy of the cluster formed in the ion/molecule reactions with C_3H_6. Therefore, we may presume the same origin for the observed selectivity towards propyne, even if this could be ascertained only by the theoretical study.

Acknowledgements

The authors wish to thank the Università degli Studi di Torino and the Italian MIUR for financial support through the 'Cofinanziamento di Programmi di Ricerca di Rilevante Interesse Nazionale.'

References

[1] S. Petrie, D.K. Bohme, Astrophys. J. 436 (1994) 411.
[2] S. Petrie, H. Becker, V. Baranov, D.K. Bohme, Astrophys. J. 476 (1997) 191.
[3] W.D. Reents Jr., M.L. Mandich, J. Chem. Phys. 96 (1992) 4440.
[4] L. Operti, M. Splendore, G.A. Vaglio, A.M. Franklin, J.F.J. Todd, Int. J. Mass Spectrom. Ion Processes 136 (1994) 25.
[5] C.D. Stinespring, J.C. Wormhoudt, J. Cryst. Growth 87 (1988) 481.
[6] M.D. Allendorf, R.J. Kee, J. Electrochem. Soc. 138 (1991) 841.
[7] M. Speranza, Trends Organomet. Chem. 1 (1994) 35.
[8] C. Hallin, I.G. Ivanov, A. Henry, T. Eglisson, O. Kordina, E. Janzén, J. Cryst. Growth 183 (1998) 163.
[9] K.L. Williams, I.T. Martin, E.R. Fisher, J. Am. Soc. Mass Spectrom. 13 (2002) 518.
[10] P. Benzi, L. Operti, G.A. Vaglio, P. Volpe, M. Speranza, R. Gabrielli, Int. J. Mass Spectrom. Ion Processes 100 (1990) 647.
[11] I. Haller, J. Phys. Chem. 94 (1990) 4135.
[12] F. Cacace, M. Speranza, Science 265 (1994) 208.
[13] M.T. Bowers, A.G. Marshall, F.W. McLafferty, J. Phys. Chem. 100 (1996) 12897.
[14] G. Cetini, L. Operti, R. Rabezzana, G.A. Vaglio, P. Volpe, J. Organomet. Chem. 519 (1996) 169.
[15] P. Antoniotti, L. Operti, R. Rabezzana, G.A. Vaglio, P. Volpe, J.-F. Gal, R. Grover, P.-C. Maria, J. Phys. Chem. 100 (1996) 155.
[16] (a) P. Antoniotti, L. Operti, R. Rabezzana, M. Splendore, G. Tonachini, G.A. Vaglio, J. Chem. Phys. 107 (1997) 1491;
(b) P. Antoniotti, L. Operti, R. Rabezzana, G. Tonachini, G.A. Vaglio, J. Chem. Phys. 109 (1998) 10853.
[17] D. Schroeder, C. Heinemann, W. Koch, H. Schwarz, Pure Appl. Chem. 69 (1997) 273.
[18] E.M. Cruz, X. Lopez, M. Ayerbe, J.M. Ugalde, J. Phys. Chem. 101 (1997) 2166.
[19] F. Cacace, Pure Appl. Chem. 69 (1997) 227.
[20] K. Raghavachari, J. Chem. Phys. 88 (1988) 1688.
[21] T.M. Mayer, F.W. Lampe, J. Phys. Chem. 78 (1974) 2433.
[22] W.N. Allen, F.W. Lampe, J. Am. Chem. Soc. 99 (1977) 6816.
[23] S. Wlodek, A. Fox, D.K. Bohme, J. Am. Chem. Soc. 113 (1991) 4461.
[24] B.H. Boo, P.B. Armentrout, J. Am. Chem. Soc. 113 (1991) 6401.
[25] A.E. Ketvirtis, D.K. Bohme, A.C. Hopkinson, J. Mol. Struct. (THEOCHEM) 313 (1994) 1.
[26] (a) P. Antoniotti, L. Operti, R. Rabezzana, G.A. Vaglio, P. Volpe, Int. J. Mass Spectrom. 190/191 (1999) 243;
(b) C. Canepa, A. Maranzana, L. Operti, R. Rabezzana, G.A. Vaglio, Organometallics 20 (2001) 4593.
[27] P. Antoniotti, C. Canepa, L. Operti, R. Rabezzana, G. Tonachini, G.A. Vaglio, J. Phys. Chem. A 103 (1999) 10945.
[28] P. Antoniotti, C. Canepa, L. Operti, R. Rabezzana, G. Tonachini, G.A. Vaglio, J. Organomet. Chem. 589 (1999) 150.
[29] P. Benzi, L. Operti, R. Rabezzana, Eur. J. Inorg. Chem. 2000 (2000) 505.
[30] S. Calderan, L. Operti, R. Rabezzana, G.A. Vaglio, J. Mass Spectrom. 37 (2002) 155.
[31] S. Calderan, P. Carbone, L. Operti, R. Rabezzana, G.A. Vaglio, J. Mass Spectrom. 37 (2002) 1205.
[32] M. Decouzon, J.-F. Gal, P.-C. Maria, A.S. Tchinianga, personal communication.
[33] J.-F. Gal, R. Grover, P.-C. Maria, L. Operti, R. Rabezzana, G.A. Vaglio, P. Volpe, J. Phys. Chem. 98 (1994) 11978.
[34] V.G. Anicich, G.A. Blake, J.K. Kim, M.J. McEwan, W.T. Huntress Jr., J. Phys. Chem. 88 (1984) 4608.
[35] T. Su, W.J. Chesnavich, J. Chem. Phys. 76 (1982) 5183.
[36] A.A. Maryott, F. Buckley, US National Bureau of Standards Circular No. 537, National Bureau of Standards, Washington, DC, 1953.
[37] K.H. Hellwege (Ed.), Landolt-Boernstein, Numerical Data and Functional Relationship in Science and Technology, Group II, vol. 14, subvol. a, Springer, Heidelberg, 1982.
[38] E.R. Lippincot, J.M. Stutman, J. Phys. Chem. 68 (1964) 2926.